High-pressure stability of the tetragonal spinel $MgMn_2O_4$: Role of inversion

Lorenzo Malavasi,[1,*] Cristina Tealdi,[1] Giorgio Flor,[1] and Monica Amboage[2]
[1]*Dipartimento di Chimica Fisica "M. Rolla" and INSTM, V.le Taramelli 16, I-27100, Pavia, Italy*
[2]*European Synchrotron Radiation Facility (ESRF) 6, rue Jules Horowitz, BP 220, 38043 Genoble, France*
(Received 3 June 2004; revised manuscript received 15 September 2004; published 5 May 2005)

The phase stability of the $MgMn_2O_4$ spinel has been studied by means of high-pressure x-ray diffraction for pressures up to 30 GPa. Two samples with different inversion degrees have been considered. Both spinels undergo a phase transition toward an orthorhombic structure ($CaMn_2O_4$ type). As for the more inverted sample the transition pressure is at least 1 GPa lower than that of the less inverted spinel, and the volume contraction, relative compressibility, and density trends are different for the two samples, as well. These variations have been explained considering the differences in the cation distribution and electronic proprieties. Besides, a general scheme for the behavior of tetragonal spinel manganites at high pressure is suggested.

DOI: 10.1103/PhysRevB.71.174102 PACS number(s): 62.50.+p, 87.64.Bx

I. INTRODUCTION

In recent years manganese-containing oxides have received a renewed interest after the discovery, in lanthanum manganites, of extremely high magnetoresistance values. Many other phases, such as layered manganites, have been also studied since the presence of manganese ions with different oxidation states induces novel and interesting properties. Among mixed-transition-metal oxides a very interesting class of compounds are the spinels. One of the most studied is cubic $LiMn_2O_4$ which is a promising material as cathode for lithium batteries.[1] Other spinel manganites with divalent cations on the tetrahedral site, such as Mn, Zn, Cd, and Mg, display a tetragonal structure as a consequence of a strong Jahn-Teller (J-T) effect due to the presence of Mn(III) ions that fill the octahedral sites of the oxygen-ion closed-packed arrangement. Since these materials are interesting from both a fundamental and applicative point of view, we started a systematic characterisation of structural, transport, and magnetic properties of manganese spinel oxides of general formula AMn_2O_4 (A=Cd, Mg, Zn, Mn).[2–7] Their physicochemical properties are strictly connected with the cation distribution on the lattice. It is common to refer to a *normal* spinel when all the A cations are in the tetrahedral sites and all the B cations (in this case Mn) are found in the octahedral ones. When all of the A ions are placed in the octahedral sites and correspondingly half of the B ions are on the tetrahedral sites, we refer to an *inverted* spinel. Of course, all the intermediate cation distributions can be considered to give origin to a *partially* inverted spinel. The inversion degree is usually expressed by a parameter m, and as a consequence the spinel formula is written as $(A_{1-m}B_m)^{tet}[A_mB_{2-m}]^{oct}O_4$.

Among those spinel manganites we focused on the $Mg_{1-x}Mn_{2+x}O_4$ system, for $0 \leqslant x \leqslant 1$, which has been scarcely studied in the previous literature apart from some papers dealing with the study of cation distribution in the end member $MgMn_2O_4$. In this spinel the inversion process has a greater tendency to occur with respect to $ZnMn_2O_4$ and $CdMn_2O_4$; as a consequence, in the $MgMn_2O_4$ compound, part of magnesium ions can be found in the octahedral sites already at room temperature. By means of high-temperature x-ray diffraction measurements we could show that the slowly cooled to room temperature spinel has an inversion degree around 0.2 and that it then starts increasing from about 600 °C reaching a value of ~0.3 at 800 °C (Ref. 2). We also observed that as the inversion process proceeded, a progressive reduction of the tetragonal distortion arose as evidenced by the contraction of the c/a' ratio (where $a' = a\sqrt{2}$). However, the exact value of the inversion degree was determined by means of Rietveld refinement of x-ray pattern and by comparing the experimental and simulated intensity ratios between those reflections highly dependent on and those independent from the inversion, respectively.

Object of this paper is the study of the role of cation distribution in the lattice, on the HP phase stability of the of $MgMn_2O_4$ spinel. For this purpose we studied two different samples: the first has been slowly cooled (SC) down to room temperature (0.1 °C/min); the second has been quenched (QD) from 1000 °C in order to make it more inverted. To the best of our knowledge this is the first work in which the effect of the inversion degree on the HP structural features of a spinel material is taken into account.

The literature regarding the HP structural properties of spinel manganites is relatively scarce if compared to other materials. However, a detailed and thorough study of HP-XRD on the Mn_3O_4 spinel up to 38GPa (Ref. 8) and a more qualitative work on $ZnMn_2O_4$ (Ref. 9) for a pressure up to 52 GPa appeared in the past literature and will be used in the following discussion in order to try to rationalize the behavior of tetragonal spinels as a function of pressure. From these works, it turned out that both Mn_3O_4 and $ZnMn_2O_4$ undergo a phase transition by increasing the pressure but with different HP phases and transition pressures (P_T): the first spinel (Mn_3O_4) turns into an orthorhombic marokitelike phase around 10 GPa while the latter changes into a tetragonal primitive cell, with a significant reduction of the c/a parameter, around 23 GPa. In order to shed light on the HP properties of tetragonal spinel manganites, an enrichment of the available literature seems to be needed. Among the possible stable tetragonal manganites we chose the magnesium one since, with respect to all the others and as explained above, it is a partially inverted spinel.

II. EXPERIMENT

$MgMn_2O_4$ samples were synthesized by solid-state reaction starting from stoichiometric amounts of Mn_2O_3 (Aldrich, 99.999%) and MgO (Aldrich, 99.9%). Pellets were prepared from the thoroughly mixed powders and allowed to react at 1200 °C for a total time of at least 6 days during which they were regrounded and repelletized at least twice. At the last thermal treatment the pellets were cooled from 1200 to 400 °C at a rate of 0.1 °C/min and from 400 °C to room temperature (RT) at 10 °C/min. This first sample will be hereinafter referred as the slowly cooled sample and indicated with the acronym SC. The other sample employed in the x-ray diffraction study was taken from the SC batch, heated to 1000 °C for 48 h, and then quenched in an ice-water mixture. This procedure assured a "freezing" of the high-temperature cation distribution.[10,11] This second sample will be hereinafter indicated as the quenched one (QD). The estimated inversion degree for the SC sample is around 20% ($m=0.2$; see definition of m in the Introduction) while for the QD it is around 40%.

X-ray powder diffraction (XRPD) and electron microprobe analysis (EMPA) inspections were performed to check the phase purity of the obtained materials. X-ray powder diffraction patterns on the so-prepared samples were acquired on a Bruker D8 Advance diffractometer equipped with a Cu anode. EMPA measurements were carried out using an ARL SEMQ scanning electron microscope, performing at least ten measurements in different regions of each sample. According to EMPA and XRPD techniques, the above synthetic procedure produced single-phase and homogenous materials with a chemical composition in agreement with the nominal one.

The high-pressure powder diffraction experiments were carried out at the European Synchrotron Radiation Facility (ESRF) of Grenoble, France, on the ID09 beamline by employing a diamond anvil cell (DAC) with culets diameter of 350 μm. N_2 was used as the pressure transmitting medium. As for the SC sample a total of 38 patterns for pressure up to 36 GPa were recorded at intervals of about 1 GPa. For the QD sample we explored a reduced pressure interval—i.e., until 23 GPa, mainly due to a break of the metal gasket during the last pressure increase. However, as will be shown in the following discussion, the most interesting P range is the one up to about 20 GPa. The P calibration was accomplished by following the fluorescence line of a ruby excited by an Ar laser source according to the well-known correlation based on a nonlinear hydrostatic pressure scale.[12] The uncertainty on P was fixed to 0.1 GPa as previously observed by other authors on data collected at ID09.[13–15]

Diffraction images were collected at a wavelength of $\lambda = 0.41793$ Å, as determined from silicon calibration, at a sample to plate distance of 364.538 mm. Data collection required about 2 min. Pressure variation during measurements was kept small (<0.05 GPa) by allowing the system to equilibrate for at least 30 min prior to any measurements. The P values used in the data analysis are the ones determined after the XRD measurements. The angular interval of the diffraction patterns resulting from the two-dimensional (2D) integrated images ranged from 3.13° to 23.36° with an angular step of 0.0138°. The two-dimensional images of the diffraction rings were integrated into 2D patterns using the FIT2D software package.[16]

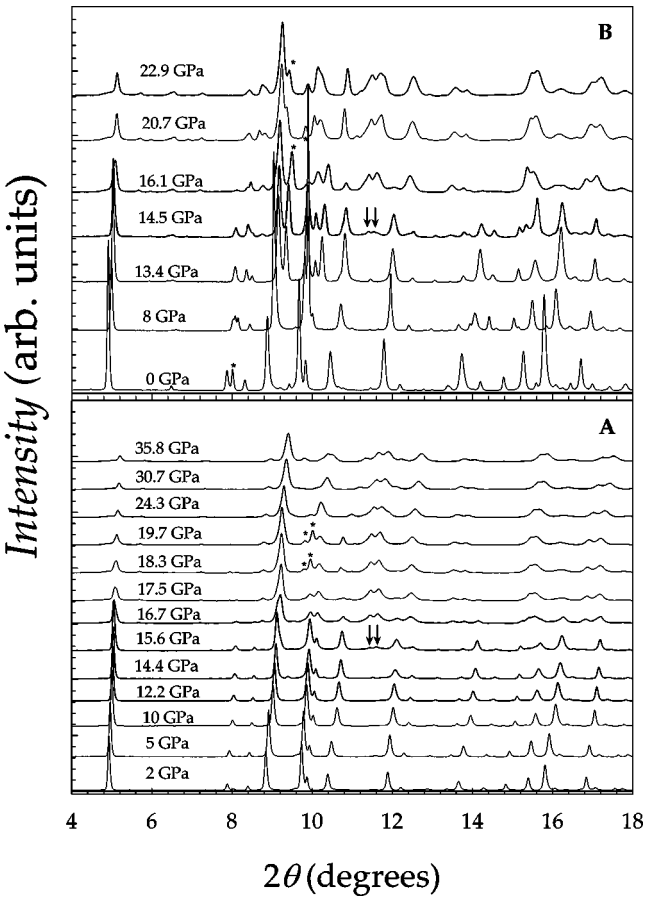

FIG. 1. X-ray diffraction patterns for the $MgMn_2O_4$ SC (A) and for the QD sample (B) at selected P values. Asterisks refer to N_2 peaks while arrows to features of the HP phase. See the text for details.

Rietveld refinements of the XRD patterns were performed by means of the FULLPROF software package.[17] The experimental patterns were modeled by a pseudo-Voigt-profile function. A first rough background fit was carried out with an exponential function on the integrated data and subtracted before the Rietveld refinements. The refined parameters were the scale factor, fifth-order polynomial background function, lattice constants, and fractional coordinates for oxygen (y and z). Thermal factors were not modeled but fixed to literature data collected on $ZnMn_2O_4$ single crystals.[9]

Equation of state analysis (EOS) was performed by means of the EOSFIT software.[18]

III. RESULTS AND DISCUSSION

Figure 1 reports some selected diffraction patterns collected on the SC sample (A, lower panel) and on the QD sample (B, upper panel) for increasing pressures values up to 35.8 GPa (SC) and 22.9 GPa (QD), respectively. As can be appreciated, around 14—16 GPa the patterns of both samples show significant changes showing the occurrence of a phase

TABLE I. Lattice constants, tetragonal distortion, and cell volume values for the $MgMn_2O_4$ SC sample at the measurements pressures.

Pressure (GPa)	a (Å)	b (Å)	c (Å)	c/a'	V (Å^3)	V (Å^3) DICVOL
0.0	5.7252(2)	5.7252(2)	9.2975(5)	1.1485(1)	304.75(3)	
2.1	5.7100(2)	5.7100(2)	9.2365(4)	1.1440(1)	301.14(3)	
2.7	5.7048(2)	5.7048(2)	9.2169(4)	1.1426(1)	299.26(3)	
4.4	5.6919(3)	5.6919(3)	9.1794(7)	1.1405(2)	297.39(5)	
5.0	5.6845(3)	5.6845(3)	9.1515(7)	1.1385(2)	295.71(5)	
5.9	5.6770(2)	5.6770(2)	9.1277(5)	1.1371(2)	294.16(4)	
6.9	5.6680(3)	5.6680(3)	9.1012(6)	1.1356(1)	292.38(5)	
8.0	5.6588(3)	5.6588(3)	9.0761(6)	1.1343(2)	290.63(5)	
9.1	5.6506(3)	5.6506(3)	9.0525(7)	1.1330(2)	289.90(5)	
10.2	5.6423(3)	5.6423(3)	9.0298(6)	1.1318(2)	287.46(5)	
11.1	5.6352(3)	5.6352(3)	9.0097(7)	1.1307(2)	286.10(5)	
12.2	5.6276(3)	5.6276(3)	8.9901(7)	1.1298(2)	284.71(5)	
13.2	5.6208(4)	5.6208(4)	8.9729(9)	1.1290(3)	283.48(6)	
14.4	5.6119(6)	5.6119(6)	8.949(1)	1.1279(3)	281.86(9)	
15.6	5.6019(6)	5.6019(6)	8.920(1)	1.1261(3)	279.92(9)	
17.5	9.383(8)	9.3870(8)	2.853(1)	-	251.3(5)	
18.9	9.325(3)	9.394(3)	2.844(1)	-	249.1(2)	
20.7	9.310(3)	9.389(3)	2.840(1)	-	248.3(2)	248.9(5)
22.6	9.282(3)	9.3769(3)	2.8346(1)	-	246.7(2)	
23.4	9.273(4)	9.371(4)	2.831(1)	-	246.0(2)	246.4(4)
24.4	9.265(3)	9.354(3)	2.827(1)	-	245.1(2)	
25.5	9.255(2)	9.344(2)	2.824(1)	-	244.2(2)	243.7(5)
27.0	9.245(3)	9.319(3)	2.819(1)	-	242.8(2)	
28.0	9.240(3)	9.307(3)	2.816(1)	-	242.2(2)	241.7(8)
29.4	9.229(3)	9.292(3)	2.813(1)	-	241.2(2)	
30.8	9.221(3)	9.275(3)	2.8092(9)	-	240.2(3)	239.8(5)
32.0	9.211(4)	9.264(3)	2.804(1)	-	239.3(3)	
33.6	9.195(4)	9.249(3)	2.798(1)	-	238.0(3)	
34.9	9.184(4)	9.230(3)	2.794(1)	-	236.8(3)	
35.8	9.173(4)	9.220(4)	2.790(1)	-	235.9(3)	235.2(6)

transition towards a high-pressure phase. All the patterns reordered from the pressure of the sample load (2 GPa for the SC sample and ~6 GPa for the QD sample) to pressure values before the transition—i.e. 15.6 GPa (SC) and 14.5 (QD)—can be satisfactorily indexed by means of a single-phase tetragonally distorted spinel belonging to the space group $I4_1/amd$ (No. 141). As can be clearly seen from the plots, the low-pressure and high-pressure phases never coexist, at least within the pressure intervals used in the experiment. However, at 15.6 GPa for the SC sample and at 14.5 GPa for the QD sample, some distinctive features of the HP phase are already seen such as, for example, the two reflections at 11.4° and 11.6° (marked with arrows in Fig. 1). At these pressure values, the main phase can be still nicely refined as a tetragonal spinel; so, afterwards, also the structural data at these P values have been used. We also stress that these two P values have been defined as the two transition pressures (P_T): 15.6 GPa (SC) and 14.5 GPa (QD), respectively.

We will first concentrate our attention to the low-pressure (LP) phases. Tables I and II show the lattice constants determined from the Rietveld refinements, the tetragonal distortion (c/a') and the cell volumes for the SC and QD samples. Up to the P_T the cell volume progressively contracts of about 7.5% (SC) and 7.6% (QD).

Figure 2 shows the lattice constants (a and c) trend versus P, while in the inset the tetragonal distortion variation as a function of pressure is plotted for the SC (open symbols) and QD (solid symbols) samples. Note that this latter parameter is defined as c/a' where $a'=a\sqrt{2}$, thus referring to the face-centered pseudocubic unit cell constructed along the diagonal of the tetragonal one. For a cubic spinel $c/a'=1$.

As can be appreciated from the inset of Fig. 2, at ambient pressure (0.000 01 GPa, hereafter indicated as $P=0$), the tetragonal distortion for the QD sample is lower of more than 2% (1.126) with respect to the SC sample (1.149). In addition, a nearly constant difference between the two samples is preserved at all the P values considered for the LP phase. A

TABLE II. Lattice constants, tetragonal distortion, and cell volume values for the $MgMn_2O_4$ QD sample at the measurements pressures.

Pressure (GPa)	a (Å)	b (Å)	c (Å)	c/a'	V (Å^3)
0.0	5.7577(2)	5.7577(2)	9.1708(4)	1.1264(1)	304.02(3)
6.3	5.6979(3)	5.6979(3)	9.0036(4)	1.1175(1)	292.30(3)
7.3	5.6856(4)	5.6856(4)	8.9769(6)	1.1166(2)	290.18(6)
8.8	5.6733(5)	5.6733(5)	8.9670(7)	1.1178(3)	288.61(7)
10.6	5.6644(5)	5.6644(5)	8.8998(7)	1.1112(3)	285.55(7)
11.8	5.6561(4)	5.6561(4)	8.8922(6)	1.1119(2)	284.47(6)
12.6	5.6498(5)	5.6498(5)	8.881(1)	1.1117(3)	283.49(8)
13.5	5.6453(5)	5.6453(5)	8.865(1)	1.1107(4)	282.54(8)
14.5	5.6356(7)	5.6356(7)	8.847(1)	1.1103(4)	281.0(1)
16.2	9.379(2)	9.486(2)	2.851(1)	-	253.7(2)
16.9	9.380(3)	9.478(3)	2.852(1)	-	253.5(2)
17.9	9.363(3)	9.454(3)	2.850(1)	-	252.3(2)
19.5	9.343(3)	9.438(3)	2.847(1)	-	251.1(2)
20.8	9.328(4)	9.436(3)	2.843(1)	-	250.3(3)
21.9	9.322(4)	9.425(3)	2.839(1)	-	249.4(3)
22.9	9.317(4)	9.415(4)	2.836(1)	-	248.8(3)

lower c/a' parameter for the more inverted sample was previously[2,10,11] interpreted as due to the inversion reaction:

$$Mg_{Mg}^{x} + 2Mn_{Mn}^{x} \rightleftarrows Mg'_{Mn} + Mn_{Mg}^{x} + Mn_{Mn}^{\bullet} \qquad (1)$$

which should reduce the Jahn-Teller induced tetragonal distortion as a consequence of the non J-T Mn(IV) formed for charge compensation.

Figure 3 reports the normalized lattice parameters (a and c) for the LP phases of both samples (SC, open symbols; QD, solid symbols). It can be noticed that the relative compressibilities along the a and c directions are at a ratio of about 1:2. This result is consistent with a progressive reduction of the tetragonal distortion as P increases. This is in turn due to the fact that the two axial (longer) Mn-O bond shortens *faster* with P than the four (shorter) equatorial Mn-O bonds. This is shown in the inset of Fig. 3 where the normalized bond lengths defined as Mn-O/Mn-O_0, where Mn-O_0 is the value at ambient pressure, are plotted as a function of P for some selected pressures.

The comparison between the normalized lattice parameters of the SC and QD samples shows that small but significant differences are present. The compressibility along the c

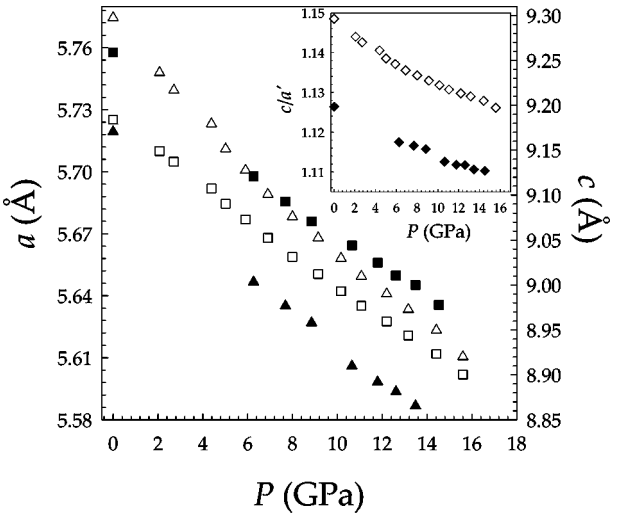

FIG. 2. Lattice constants a and b (squares) and c (triangles up) for the $MgMn_2O_4$ SC (open symbols) and QD (solid symbols) samples as a function of P. In the inset the c/a' vs P trend is reported (same conventions for symbols as main Fig. 2).

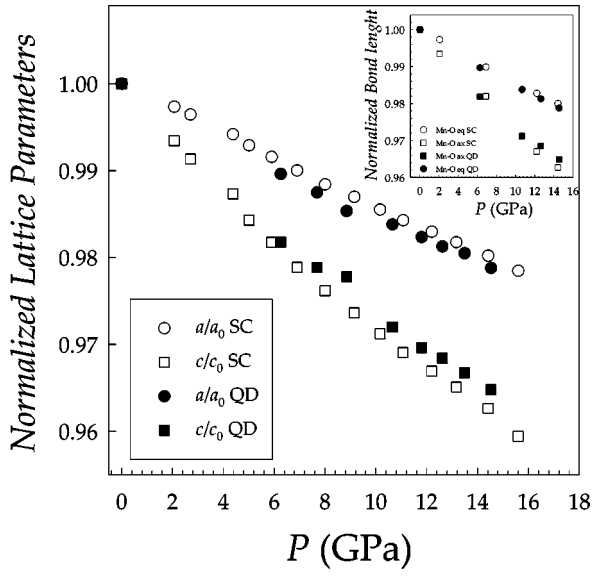

FIG. 3. Normalized lattice constants for $MgMn_2O_4$ SC sample (open symbols) and QD sample (solid symbols). Circles: a. Squares: c. The inset reports the behavior of normalized bond lengths for both samples. Squares: axial Mn-O bond. Circles: equatorial Mn-O bond.

axis slightly reduces while the one along the *a* axis increases by increasing the inversion degree. Let us note that in the case of a cubic structure no differences between the three directions should be present. So this result can be directly connected to the increased inversion in the spinel and in the change of cation occupancies between the tetrahedral and octahedral structural sites.

Finally, the theoretical density of the spinels, calculated from the lattice constants, increases of about 8.9% from ambient pressure ($d=4.319\ \mathrm{g/cm^3}$) to 15.6 GPa ($d=4.702\ \mathrm{g/cm^3}$) for the SC sample and of about 8.2%, from $d=4.330\ \mathrm{g/cm^3}$ at 0 GPa to $4.681\ \mathrm{g/cm^3}$ at 14.5 GPa, for the QD sample.

Let us now switch to the HP phases. By reviewing the current literature concerning high-pressure structural studies of spinel oxides, the presence of a HP-distorted structure proves to be a general characteristic of the spinel structure both for the cubic and tetragonal symmetry.[14,19–22] The most common high-pressure structures (all orthorhombic) are the $CaFe_2O_4$ (space group *Pnma*, No. 62), $CaTi_2O_4$ (space group *Cmcm*, No. 63), and $CaMn_2O_4$ (space group *Pmab*, No. 57) structures. However, among the works cited, only one relates to spinel manganites and particularly to the Mn_3O_4 (Ref. 22) compound. In that work the authors found that the orthorhombic phase formed at high-pressure possesses a structure similar to the one of marokite ($CaMn_2O_4$) but with significant differences due to the replacement of Mn(II) for Ca(II). The only other structural report about tetragonal spinels behavior at HP is the one recently due to Wang *et al.*[20] which is devoted to the study of $CoFe_2O_4$. For this spinel the stable HP phase is the $CaFe_2O_4$ one, mainly due to the chemical similarity between the two compounds. We remark that the differences between the three orthorhombic structures reported above are relatively small and in some cases it turned out that an unambiguous distinction between them was not possible mainly due to the relatively low quality of the x-ray data.[14]

For completeness' sake we tested all the three possible structures by refining the patterns where only the new HP phase is present—i.e., from 17.5 GPa for the SC sample and from 16.2 GPa for the QD one up to the highest *P* values explored for both samples, with the three different starting models. This kind of test demonstrated that the best agreement between the observed and calculated patterns was achieved when considering the $CaMn_2O_4$ structure ($R_p=7.2$) as the starting model. In particular, a satisfactory refinement of the patterns was not possible with the $CaFe_2O_4$ structure. The lattice constants for the HP phase of the SC and QD samples are also reported in Tables I and II, respectively.

A graphical representation of the HP phase of $MgMn_2O_4$ is presented in Fig. 4. In this structure the coordination number of *A* cations is increased to 8, with respect to the tetrahedral coordination in the spinel, while the *B* ions retain their octahedral coordination. However, as it can be seen from Fig. 4, this structure is dominated by edge-sharing strips of octahedral *B* ions running parallel to the *c* axis. These strips are two octahedra wide and are linked into a herringbone pattern, thus giving origin to triangular channels in which the

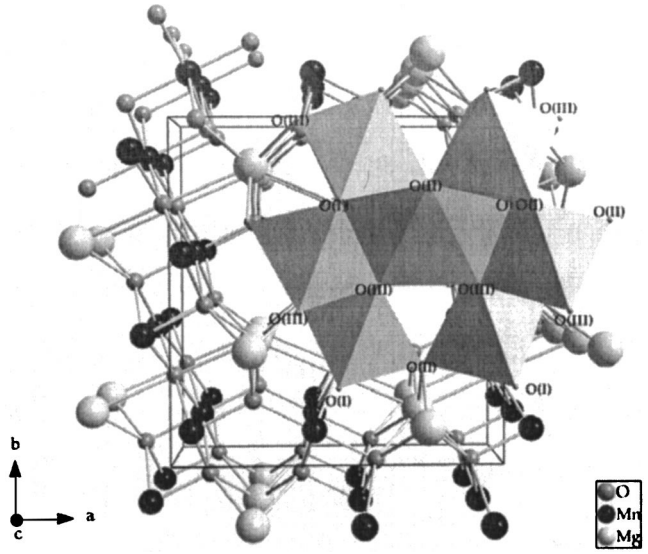

FIG. 4. Graphical representation of the HP structures of the $MgMn_2O_4$ spinel.

A ions are irregularly coordinated to eight oxygens with six different bond lengths. Also the octahedral environment is relatively distorted with six different bond lengths.[22]

Table III reports, as selected examples, the bond lengths for the tetragonal SC and QD samples at ambient pressure, at a *P* close to P_T (14.4 and 14.5 GPa) and in the orthorhombic phase (at 18.81 and 30.7 GPa for the SC sample and 19.5 GPa for the QD sample) calculated from the lattice constants determined at different pressures.

We wish to point out that in all the refinements, both at low and high pressure, we always kept the fractional occupancies of the cations fixed to those previously determined[2] since the quality of the data and, for the HP measurements, the peaks broadening due to stress effects limited the amount of information that could be extracted from the Rietveld refinements.

Figure 5 reports the cell volume variation in the whole *P* range explored for the SC (open symbols) and QD (solid symbols) samples. At the phase transition, considered to be about 2 GPa wide—i.e., from 15.6 GPa to 17.5 GPa—the cell of the SC sample contracts of 10.2% and the bulk density increases from 4.70 to $5.24\ \mathrm{g/cm^3}$(+11.4%). For the QD sample, across the transition, the theoretical bulk density increases of about 10.7% from $4.694\ \mathrm{g/cm^3}$ (14.5 GPa) to $5.187\ \mathrm{g/cm^3}$ (16.2 GPa) while the volume contraction is around 9.5%. These results indicate that the unit cell of the QD sample contracts of nearly 0.7% less than the SC sample. This can be mainly connected to the more "compacted" structure of the first sample (QD) due to an overall reduction of distortion as a consequence of a different ion distribution in the structure caused by the greater inversion.

In comparison, in the Mn_3O_4, at the P_T, which is between 10 and 12 GPa, the volume reduces of 8.6% (Ref. 8). Besides, before the phase transition, the *V* contracts of about 8.15% from 0 to 15.6 GPa and of 4.7% for an analogous *P* range (from 17.5 to 32 GPa) in the HP phase. Figure 5 shows some additional points (crossed circles) relative to volume values at HP: these values (referred to the SC sample) have

TABLE III. Bond lengths at selected P values for the two samples considered.

$MgMn_2O_4$ SC LP phase	$P=0$	$P=14.4$ (GPa)	$MgMn_2O_4$ SC HP phase	$P=18.8$ (GPa)	$P=30.7$ (GPa)
A-O	1.99(1) Å	1.94(3) Å	*A*-O(I)	2.53(6)(2×)	2.50(8)(2×)
B-O (×2)	2.25(2) Å	2.16(6) Å	*A*-O(II)	2.01(5)	1.99(9)
B-O (×4)	1.93(1) Å	1.89(5) Å	*A*-O(II)	2.04(7)	2.01(8)
			A-O(III)	2.24(7)(2×)	2.2(1)(2×)
			A-O(III)	2.17(7)(2×)	2.14(9)(2×)
			B-O(I)	2.18(6)	2.16(9)
			B-O(I)	1.85(6)	1.83(8)
			B-O(II)	1.86(5)	1.84(8)
			B-O(III)	1.83(6)	1.81(9)
			B-O(III)	2.20(6)	2.17(8)
			B-O(III)	1.86(8)	1.84(8)
$MgMn_2O_4$ QD LP phase	$P=0$	$P=14.5$ (GPa)	$MgMn_2O_4$ QD HP Phase	$P=19.5$ (GPa)	
A-O	1.99(2) Å	1.94(4) Å	*A*-O(I)	2.54(6)	
B-O (×2)	2.22(2) Å	2.14(7) Å	*A*-O(II)	2.02(5)	
B-O (×4)	1.94(1) Å	1.90(4) Å	*A*-O(II)	2.04(6)	
			A-O(III)	2.24(7)(2×)	
			A-O(III)	2.17(5)(2×)	
			B-O(I)	2.19(7)	
			B-O(I)	1.86(5)	
			B-O(II)	1.86(6)	
			B-O(III)	1.86(5)	
			B-O(III)	2.20(8)	
			B-O(III)	1.86(6)	

not been determined through the Rietveld refinement but by means of DICVOL software[23] which, basically, makes an automatic indexing of the powder pattern. From this procedure it turned out that the best final solution based on our patterns was an orthorhombic cell with lattice parameters in agreement, within the estimated standard deviation, with the ones determined from the Rietveld refinement based on a *Pmab* structure.

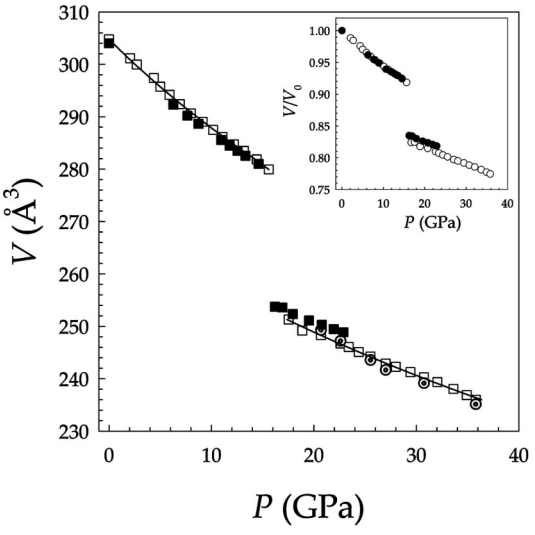

FIG. 5. Cell volume variation for $MgMn_2O_4$ SC sample (open squares) and for QD sample (solid symbols). Lines represent the EOS fit. Crossed circles are volume data determined by means of DICVOL software.

The V vs P data presented in Fig. 5 were used to calculate the bulk modulus $[K=-V(\partial P/\partial V)]$ of the samples for both the LP and HP structures. The data were fitted according to the Murnaghan EOS

$$P=\frac{K_0}{K_0'}\left[\left(\frac{V_0}{V}\right)^{K_0'}-1\right], \tag{2}$$

where K_0 is the bulk modulus at $P=0$ while K' is the first derivative of the bulk modulus versus P, respectively. To treat our data we fixed the K' value to 4. This procedure was chosen because (i) the correlation between the fitting parameters (V_0, K_0, and K') was too high if K' was also considered in the refinement thus giving origin to misleading results; (ii) it was applied by all the other authors who dealt with HP-XRD on tetragonal spinels, thus making more meaningful a comparison between ours and previous data.

For the LP phase the K_0 value was 156.0±0.7 GPa ($\chi^2=2.38$) for the SC sample and 155.1±1.2 GPa ($\chi^2=6.2$) for the QD sample. So even within the limit of a relatively low estimated difference of the inversion degree between the two

samples (around 20%) we can state that the overall compressibility behavior does not change significantly with the inversion degree.

Concerning the HP phase the estimation of the EOS was done only for the SC sample since for the second one the result obtained was not reliable mainly due to the low amount of HP data available with respect to the SC sample. As for the latter, the bulk modulus of the orthorhombic HP phase increases to 196±4 GPa ($\chi^2=3.4$) with $V_0=270.67$ Å^3 (in this case also this parameter was refined).

In comparison, in Mn_3O_4, $K_0=134.0\pm3.7$ GPa for the tetragonal phase and 166.6±2.7 GPa for the HP marokitelike structure.[8] As for $ZnMn_2O_4$, $K_0=197\pm5$ GPa, by considering V vs P data up to only 12 GPa (Ref. 9). In addition, also the tetragonal $MgFe_2O_4$ spinel undergoes a transformation towards an orthorhombic $CaTi_2O_4$-like phase between 23.7 and 32.4 GPa (Ref. 20) and K_0 increases from 94±12 GPa (tetragonal phase) to 145 GPa (orthorhombic phase). Finally, for most of the cubic spinels which become orthorhombic at HP the differences between the LP and HP phases, in term of bulk modulus and density, are smaller then the tetragonal spinels; for example, the HP structures are generally only 2%–3% denser than the cubic LP ones. This smaller difference between the HP and LP polymorphs is reasonable since the cubic structure is more compact than the tetragonal one for which, in fact, the density variation between the two polymorphs is significantly larger.

Finally, in order to highlight the difference in the V vs P trend for the two samples, we reported, in the inset of Fig. 5, the normalized volumes for both spinels: open squares represent the data for the SC sample while the solid symbols are relative to the QD one.

As regards the transition pressure values (P_T) we note that for the QD sample the new HP phase is already appreciable present (few percent of phase detected) at 14.5 GPa, a pressure value at which, on the contrary, no traces of the new phase are detectable for the SC sample. The first evidence of the formation of the HP phase for the SC sample appears in the pattern recorded at 15.6 GPa. Moreover, at this P value the amount of the new HP phase for the SC sample can be considered roughly equal to the amount found at 14.5 GPa in the QD sample. Even though the P interval between two successive measurements is not narrow enough to look at detailed differences in the P_T values, the above reported evidences indicate that the HP phase is formed before for the QD sample with respect to the SC sample of at least 1 GPa.

The presence of a phase transition towards an orthorhombic phase in the $MgMn_2O_4$ spinels for both cation distributions, as found for the Mn_3O_4 (Ref. 8) and contrary to the $ZnMn_2O_4$ spinel (Ref. 9), is a first significant result found in this work.

Thanks to our data, which enrich the available literature, we try to discuss some remarkable aspects of tetragonal spinel manganites at HP: namely, (i) a phase transition towards a more distorted structure and not towards a more regular one [as found in a great variety of JT systems at HP (Refs. 24–26)] together with its dependence on the samples features; (ii) the differences in behavior between the three members of tetragonal spinel manganites family for which HP data are now available.

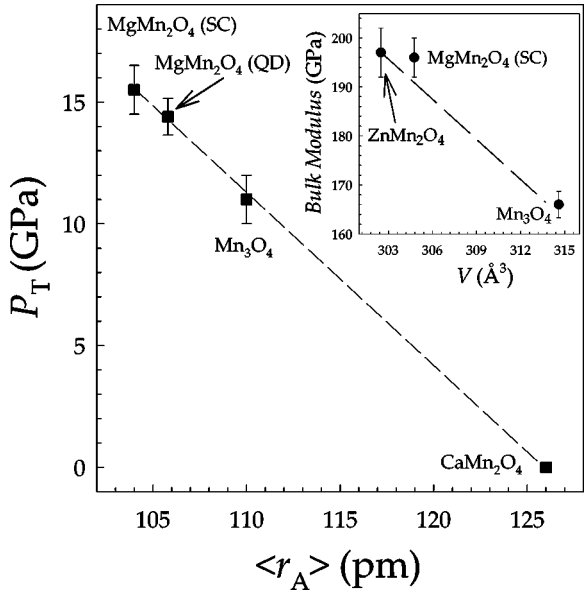

FIG. 6. Transition pressures for various spinel manganites (see names in the plot) vs the average ionic radius of the A site. Inset: bulk modulus values vs cell volumes.

It has been pointed out[22] that the ionic radius of Mn(II) is too small to achieve the eightfold coordination already found at ambient pressure in the marokitelike phase already. Figure 6 displays the average ionic radius of the A site, $\langle r_A\rangle$, for Mn_3O_4 and $MgMn_2O_4$ (SC and QD samples) against the transition pressure from the tetragonal to the orthorhombic marokitelike phase. For $CaMn_2O_4$ this value was set equal to 0 since the orthorhombic phase is already stable at ambient P. The graph can be also interpreted as the pressure range of stability of the $CaMn_2O_4$ phase as a function of the A-ion dimension. This dependence may also explain the difference in the P_T between the SC and QD $MgMn_2O_4$ samples: the average ionic radius on the A site is greater for the more inverted spinel, which allows the $I4_1/amd \rightarrow Pmab$ transition to occur at a pressure of at least 1 GPa lower with respect to the less inverted sample (SC). So, apparently, for those spinels which undergo this kind of phase transition the pressure at which this happens is mainly controlled by the ionic radii and consequently by the ions distribution between the tetrahedral and octahedral sites, as nicely shown for the two $MgMn_2O_4$ samples.

However, the fact that Mn_3O_4 and $MgMn_2O_4$ spinels undergo a phase transition towards a more distorted structure, with respect to the ambient pressure tetragonal one, by increasing P, is quite remarkable. One could expect that the application of an external P would increase the orbital degeneracy and stabilize the $t_{2g}^4(\uparrow\downarrow\uparrow\uparrow)$ LS configuration with respect to the HS configuration $t_{2g}^3(\uparrow\uparrow\uparrow)e_g^1(\uparrow)$, thus leading to the removal of the Jahn-Teller distortion and to the appearance of a cubic crystal symmetry. However, this is never the case, not even for the $ZnMn_2O_4$ spinel which remains tetragonal at HP. In addition, not only is a cubic symmetry not achieved, but the axial distortion increases as confirmed by the bond-length differences between the four equatorial and two axial bonds which rises in the HP phase of at least 0.1 Å.

This suggests that the on-site Hund energy gained by the degeneracy removal is always greater than the Δ_0 and that the Jahn-Teller energy term is always favorable and (possibly) increases by increasing P. In other term, it is the J-T effect that prevents the system from undergoing a HS-LS transition which, in absence of that, will lead to an energy gain. Moreover, as a consequence of the strong J-T effect we expect these tetragonal spinels to display a strong electron-lattice coupling, which had been already observed in other systems to increase by increasing the applied P (Ref. 27). What can be imagined is the this effect should give origin to an increase of the J-T energy term, thus making an increase of the axially distortion more pronounced. Noteworthy, the evolution, at HP, towards a highly distorted structures is shown by those two samples which present, already at ambient pressure, the highest tetragonal distortion: namely, Mn_3O_4 ($c/a'=1.162$) and $MgMn_2O_4$ ($c/a'=1.148$ SC) while $ZnMn_2O_4$ is around 1.143. However, let us note that for the $MgMn_2O_4$ spinel this value is mediated also over some non J-T octahedra, where the Mn(IV) ions are present (around 10% of the total) which influence the lattice parameter but probably they do not affect strongly the setup of a cooperative J-T effect. This is also true for the QD sample ($c/a'=1.126$ SC) where the role played by the majority of J-T octahedra should dominate the structural features at HP. So it can be expected that a lower distortion at ambient P connected to a lower electron-lattice coupling could effectively reduce the J-T effect by increasing P over the whole P range explored and that this could make also available to the electrons the occupancy of x^2-y^2e_g states and lead to a strong reduction of the tetragonal distortion, as observed by Åsbrink *et al.*[9] On the contrary, for more distorted structures, the faster increase of the *e-p* coupling with P, with respect to the reduction of the distortion (which is evident for pressures up to the P_T), makes the increase of the $E_{J\text{-}T}$ always greater, thus provoking a distortion of the structure at HP. It seems also that this aspect is closely related to another structural one—i.e., the relative sizes of the A ions. The definition of which phase is stable at HP and for which value the phase transition occurs is likely to be due to the combination of these two related aspects.

In the inset of Fig. 6 we reported the trend of K_0 versus the cell volumes. Values for Mn_3O_4 and $ZnMn_2O_4$ have been taken from the literature.[8,9] The bulk moduli reported in Fig. 6 for Mn_3O_4 and $MgMn_2O_4$ are those of the HP structures in order to compare them with the $ZnMn_2O_4$ data. As can be observed, the data follow a roughly linear trend, thus obeying the empirical predictions of constant K_0-V_0. Let us remember that a reliable value for the QD $MgMn_2O_4$ bulk modulus was not determined and so this does not appear in Fig. 6. In addition, the tendency of tetragonal spinel manganites to move towards K_0 values close to the ones found for HP polymorphs of cubic spinels—i.e., around 200 GPa (Ref. 19)—can be noticed.

IV. CONCLUSION

In this paper we reported the results of a high-pressure x-ray diffraction study for the tetragonal $MgMn_2O_4$ spinel for two samples with different inversion degrees. The main found results are the following.

(i) $MgMn_2O_4$ spinels, at both cation distributions, undergo a phase transition at HP towards an orthorhombic phase of $CaMn_2O_4$-type.

(ii) A correlation between the average ionic radius of the A site, $\langle r_A \rangle$, and the transition pressures from the tetragonal to the orthorhombic marokitelike phase has been found.

(iii) The bulk moduli for the spinels follow a roughly linear trend, thus obeying the empirical predictions of constant K_0-V_0. The tendency of tetragonal spinel manganites is to move towards K_0 values close to the ones found for HP polymorphs of cubic spinels—i.e., around 200 GPa.

(iv) A *tetragonal* → *orthorhombic* transition occurs at lower pressure for the more inverted sample and with lower V and density contraction at the transition pressure.

(v) By increasing the spinel inversion, lower differences in the relative compressibility of lattice directions are detected.

ACKNOWLEDGMENTS

The authors acknowledge the support of ESRF and the Ministry of Research for partial financial support through the PRIN-2004. Professor G. Bendelli is gratefully acknowledged for her critical review of language and style.

*Electronic address: lorenzo.malavasi@unipv.it

[1] G. Amatucci and J-M. Tarascon, J. Electrochem. Soc. **149**, K31 (2002).
[2] L. Malavasi, P. Ghigna, G. Chiodelli, G. Maggi, and G. Flor, J. Solid State Chem. **166**, 171 (2002).
[3] L. Malavasi, P. Galinetto, M. C. Mozzati, C. B. Azzoni, and G. Flor, Phys. Chem. Chem. Phys. **15**, 3876 (2002).
[4] L. Malavasi, M. C. Mozzati, G. Chiodelli, C. B. Azzoni, and G. Flor, J. Mater. Sci. **39**, 1671 (2004).
[5] P. Ghigna, G. B. Barbi, G. Chiodelli, G. Spinolo, L. Malavasi, and G. Flor, J. Solid State Chem. **153**, 231 (2000).
[6] C. B. Azzoni, M. C. Mozzati, L. Malavasi, P. Ghigna, and G. Flor, Solid State Commun. **119**, 591 (2001).
[7] C. B. Azzoni, M. C. Mozzati, P. Ghigna, L. Malavasi, and G. Flor, Solid State Commun. **117**, 511 (2001).
[8] E. Paris, C. R. Ross, and H. Olijnyk, Eur. J. Mineral. **4**, 87 (1992).
[9] S. Åsbrink, A. Waskowska, L. Gerward, J. Staun Olsen, and E. Talik, Phys. Rev. B **60**, 12 651 (1999).
[10] N. K. Radhakrishnan and A. B. Biswas, Phys. Status Solidi A **37**, 719 (1976).
[11] R. Manaila and P. Pausescu, Phys. Status Solidi **9**, 385 (1965).
[12] H. K. Mao, J. Xu, and P. M. Bell, J. Geophys. Res. **91**, 4673 (1986).

[13] A. Pavese, D. Levy, and V. Pischedda, Eur. J. Mineral. **13**, 929 (2001).
[14] D. Levy, A. Pavese, and M. Hanfland, Phys. Chem. Miner. **27**, 638 (2000).
[15] D. Levy, A. Pavese, A. Sani, and V. Pischedda, Phys. Chem. Miner. **28**, 612 (2000).
[16] A. P. Hammersley, S. O. Svensson, M. Hanfland, A. N. Fitch, and D. Hausermann, High Press. Res. **14**, 235 (1996).
[17] J. Rodriguez-Carvajal, Physica B **192**, 55 (1993).
[18] R. J. Angel, in *High-Pressure, High-Temperature Crystal Chemistry*, edited by R. M. Hazen and R. T. Downs [Rev. Mineral. Geochem.**41**, 35 (2001)].
[19] D. Levy, A. Pavese, and M. Hanfland, Am. Mineral. **8**, 93 (2003).
[20] Z. Wang, R. T. Downs, V. Pischedda, R. Shetty, S. K. Saxena, C. S. Zha, Y. S. Zhao, D. Schiferl, and A. Waskowka, Phys. Rev. B **68**, 094101 (2003).
[21] D. Levy, V. Diella, M. Dapiaggi, A. Sani, M. Gemmi, and A. Pavese, Phys. Chem. Miner. **31**, 122 (2004).
[22] C. R. Ross II, D. C. Rubie, and E. Paris, Am. Mineral. **75**, 1249 (1990).
[23] A. Boultif and D. Louer, J. Appl. Crystallogr. **24**, 987 (1991).
[24] P. Postorino, A. Congeduti, P. Dore, A. Sacchetti, F. Gorelli, L. Ulivi, A. Kumar, and D. D. Sarma, Phys. Rev. Lett. **91**, 175501 (2003).
[25] P. Postorino, A. Congeduti, E. Degiorgi, J. P. Itie, and P. Munsch, Phys. Rev. B **65**, 224102 (2002).
[26] A. Congeduti, P. Postorino, E. Caramango, M. Nardone, A. Kumar, and D. D. Sarma, Phys. Rev. Lett. **86**, 1251 (2001).
[27] F. Aguado, F. Rodriguez, and P. Nunez, Phys. Rev. B **67**, 205101 (2003).